UNIVERSITÀ
degli STUDI
di CATANIA

DEPARTMENT OF CLINICAL AND EXPERIMENTAL MEDICINE
PHD COURSE "BIOMEDICINA TRASLAZIONALE (36° CICLO)"
COORDINATOR: CHIAR.MO PROF. CARLO VANCHERI

PhD Thesis

Diagnostic and prognostic application of the CircSMARCA5-SRSF1 molecular axis in diffuse and circumscribed gliomas of the adults

PhD Candidate
Dr. Giuseppe Broggi

Supervisor:
Chiar.mo Prof. Rosario Caltabiano

Anno Accademico 2022-2023

Summary

1. Introduction

The generic term "glioma" indicates a wide group of tumors of the central nervous system (CNS) arising from the glial component of CNS tissue that has a support and nutrition function for neurons [1,2]. Classically, based on the supposed specific cellular type of origin, gliomas are subclassified into astrocytomas, oligodendrogliomas, ependymomas, mixed gliomas (i.e. oligoastrocytomas) and other rarer subtypes, such as brain stem gliomas [3-5]. Gliomas are the second most common tumors of the CNS [6,7]. According to the fifth edition of the World Health Organization (WHO) Classification, they are distinguished on the basis of their growth pattern, into “diffuse”, which diffusely infiltrate the surrounding nervous tissue, and "circumscribed”, which rather display a more contained growth [7]; the clinical relevance of this distinction lies in the fact that circumscribed gliomas can be cured by surgical resection. Conversely, due to their intrinsic infiltrating nature, diffuse gliomas tend to recur after surgery and may require adjuvant treatment. The fifth WHO edition further classifies diffuse gliomas into “adult-type” and “pediatric-type”, first emphasizing that diffuse gliomas primarily occurring in adults and those primarily occurring in children exhibit distinct clinical and molecular features [7]. Because of the significant favorable prognostic value of IDH mutations and 1p/19q codeletion in diffuse gliomas in adults, they have been classified as: astrocytoma IDH-mutant, oligodendroglioma IDH-mutant and 1p/19q-codeleted, and glioblastoma IDH-wild type (GBM IDHwt) [7]. According to specific histopathological or molecular features, astrocytoma IDH-mutant is graded as CNS WHO grade 2, 3, or 4, oligodendroglioma IDH-mutant and 1p/19q-codeleted as CNS WHO grade 2 or 3,

while GBM IDHwt is classified as CNS WHO grade 4 [7]. Therefore, differently from the previous classification (2016), the designation of “glioblastoma” is now reserved to IDH-wild type tumors, whereas astrocytic IDH-mutant tumors with histologically worrisome features (microvascular proliferation and/or necrosis) are classified as IDH-mutant astrocytomas, CNS WHO grade 4 [7,8]. IDH mutations were first identified in diffuse gliomas in 2008 [6-16]. IDH1/IDH2 mutations determine a gain of function phenotype to the corresponding encoded proteins that lead to the 2-hydroxyglutarate overexpression [17]; this oncometabolite, through the induction of cytosine-phosphate-guanine (CpG) island methylator phenotype (G-CIMP), lead to diffuse hypermethylation in gene promoter regions, silencing the expression of multiple cellular differentiation factors and promoting glioma onset Approximately 90% of IDH-mutant diffuse gliomas harbor the IDH1 p.R132H mutation[7,8], which can be detected via immunohistochemistry using a specific antibody. Of the remaining 10%, 5% displayed other mutations in IDH1 at residue R132, and 5% displayed mutations in IDH2 at residue R172 [8]. DNA sequencing is required to identify IDH2 and IDH1 mutations that differ from p.R132H (so-called “non-canonical IDH mutations) [8]. Over the last decade, a novel diagnostic approach, as an alternative to histopathology, has been used for tumors of the central nervous system. This is based on the concept that different tumor types harbor distinct DNA methylation profiles depending on their cell of origin and the molecular alterations that they acquire during tumorigenesis [7,8]. In 2018, CNS tumors were distinguished in 82 methylation classes [8]. The methylation class family glioma IDH-mutant included three subclasses: i) subclass astrocytoma (mainly including tumors histologically classified as CNS

WHO grade 2 or 3); ii) subclass high-grade astrocytoma (mostly formed of tumors histologically classified as CNS WHO grade 3 or 4); and iii) subclass 1p/19q codeleted oligodendroglioma. Other subtypes with distinct DNA methylation profiles have been recently described.

2. Astrocytoma, IDH-mutant [7-35]

The majority of IDH-mutant astrocytomas are localized in the supratentorial compartment, and specifically in the frontal lobes, similar to oligodendrogliomas IDH-mutant and 1p/19q codeleted. Although a subset of tumors may localize to the infratentorial compartment, they represent a molecularly distinct tumor type, which is discussed in a separate section of this review. IDH-mutant astrocytomas mainly affect young adults, with a median age of 37 years at diagnosis. According to the fifth edition of the WHO Classification, this is defined as a diffusely infiltrating IDH1- or IDH2-mutant glioma with frequent ATRX and/or TP53 mutations and the absence of 1p/19q codeletion (which instead characterizes oligodendroglioma). Therefore, the mere presence or absence of specific genetic features defines this tumor type, whereas a diffuse growth pattern represents the only histological diagnostic criterion. However, while the mutation at codon 132 of IDH1 or codon 172 of IDH2 is an essential diagnostic criterion, demonstrating the absence of 1p/19q codeletion is not necessary in cases showing ATRX mutations or the immunohistochemical loss of ATRX protein. ATRX encodes a chromatin-binding protein that acts as epigenetic and functionality regulator for telomeres. Particularly, its absence seems to induce an abnormal telomere maintenance mechanism called "*alternative lengthening of telomeres*" (ALT), able

to preserve neoplastic cells from senescence. Interestingly, ATRX loss is mutually exclusive with mutations of telomerase reverse transcriptase (TERT) gene, which induce the activation of cellular immortality mechanism mediated by telomerases, found instead tipically in IDH-mutant and 1p/19q codeleted oligodendrogliomas and IDH-wild type GBMs.

It should be emphasized that the assessment of ATRX immunostaining should always consider the endothelial or other non-neoplastic cells that serve as internal positive controls for the immunoreaction. ATRX mutations determine genomic instability and p53-dependent cellular death; consequently, TP53 mutations in IDH-mutant astrocytomas enables cell survival in the context of ATRX deficiency. Immunohistochemical staining of p53 protein is commonly used in routine practice as a surrogate for TP53 mutation; indeed, immunopositivity of >10% tumor nuclei is considered to predict the presence of TP53 mutations with a high diagnostic accuracy. Therefore, strong widespread immunostaining for p53 supports the diagnosis of astrocytoma IDH-mutant in the differential towards oligodendroglioma IDH-mutant and 1p/19q codeleted. Histologically, IDH-mutant astrocytomas may range from well-differentiated, low-density and lowly proliferative tumors to anaplastic, hypercellular and highly proliferating tumors. Their histopathological features, together with genetic features consisting of the homozygous deletion (HD) of CDKN2A/B, are used as criteria for grading these tumors. Astrocytoma IDH-mutant CNS WHO grade 2 is defined as an infiltrative tumor, with a mild to moderate cellularity, lacking microvascular proliferation, necrosis, and CDKN2A/B HD, which is composed of glial cells with mild nuclear atypia, oval hyperchromatic nuclei and absent or uncommon mitoses. Compared

to CNS WHO grade 2, astrocytoma IDH-mutant CNS WHO grade 3 features higher tumor density, even focal anaplasia, and significant mitotic activity. Although the cut-off of mitoses distinguishing CNS WHO grade 2 and 3 astrocytomas IDH-mutant has not been established, one mitosis is sufficient for the designation of grade 3 in small biopsies, whereas more are required in larger specimens. Finally, IDH-mutant astrocytoma is classified as CNS WHO grade 4 in the presence of microvascular proliferation and/or necrosis and/or CDKN2A/B HD. The latter has been incorporated as a criterion for grading astrocytomas IDH-mutant in the fifth WHO edition because tumors histologically defined as grade 3 and showing this genetic abnormality had a clinical course corresponding to that of grade 4 tumors. According to the WHO classification, an astrocytoma IDH-mutant with histological features consistent with CNS WHO grade 2 is diagnosed as CNS WHO grade 4 if CDKN2A/B HD is present. Therefore, the analysis of CDKN2A/B HD is mandatory for the proper grading of these tumors, according to the WHO. CDKN2A/B HD can be identified using fluorescence in situ hybridization (FISH), methylation profiling, or next-generation sequencing. All these techniques have several limitations and require expert personnel to interpret the results. FISH analysis is carried out using two probes: one that hybridizes to chromosome 9 centromeric sequences, and another that covers a region of 9p that includes CDKN2A, CDKN2B, and MTAP genes. Therefore, FISH may give false-positive results in cases with deletions smaller than the region covered by the 9p probe. In addition, there is currently no consensus on the cut-off for nuclei with CDKN2A/B HD required to define the presence of this genetic alteration. In a study of 121 IDH-mutant astrocytomas using FISH and a cut-off of 30% deleted

nuclei, CDKN2A/B HD was found in 1.8%, 3.2% and 27% of cases histologically classified as grade 2, 3 or 4. Notably, this genetic alteration was significantly associated with a worse prognosis only in tumors histologically classified as grade 4 (i.e. with microvascular proliferation and/or necrosis) and this result was invariable using a cut-off value of 10% or 20% nuclei with CDKN2A/B HD. Another study, using FISH and a cut-off of 10% nuclei, did not find CDKN2A/B in any of the 15 analyzed IDH-mutant astrocytomas histologically classified as grade 2. In the Tumor Cancer Genome Atlas (TCGA) merged cohort of lowgrade gliomas and glioblastomas (accessible at www.cbioportal.org), we found CDKN2A/B HD in 4/110 (3.6) and in 7/102 (7%) IDH-mutant astrocytomas histologically defined as grade 2 or 3. CDKN2A/B HD was significantly associated with shorter patient overall survival in the latter (P=0.0229), but not in the former (P=0.161). Therefore, CDKN2A/B seems to be rare in IDH-mutant astrocytomas histologically classified as grade 2 and its prognostic value in this setting probably needs further confirmation. CDKN2A encodes for the p16 protein; however, whether the immunohistochemical loss of p16 correlates with CDKN2A homozygous deletion is controversial. Therefore, the p16 immunohistochemical assessment is not recommended as a surrogate for CDKN2A homozygous deletion. Since MTAP is located on chromosome 9p21, only 165kb telomeric to CDKN2A, and it is often deleted simultaneously with CDKN2A in tumors, immunohistochemical loss of MTAP protein has been recently proposed as a surrogate for CDKN2A/B homozygous deletion. Although further studies are needed to validate its use in clinical practice, the loss of MTAP seems to predict CDKN2A/B with a high sensitivity (88%) and specificity (98%).

Although the morphology of histologically defined astrocytomas IDH-mutant CNS WHO grade 4 was traditionally considered overlapping with that of glioblastoma IDH-wildtype, some differences exist between these tumor types. Indeed, zonal and/or palisading necrosis is considerably more frequent in IDH-wild type glioblastoma than in IDH-mutant astrocytoma CNS WHO grade 4 (90% vs 50%) (Nobusawa et al., 2009). In addition, the latter features significantly more TP53 (96.2% vs 27%) and ATRX (76.9% vs 4.6%) mutations and less frequent EGFR amplification (0% vs 46.3%), CDKN2A/B HD (16.7% vs 57.7%) and PTEN alterations (4.2% vs 33.9%).

3. Glioblastoma, IDH-wild type (WHO grade 4) [36-43]

GBM is a malignant glioma with astrocytic differentiation, characterized by high-grade histological features, necrosis and/or microvascular proliferation in absence of mutations of IDH1/2 genes. WHO assigns a histological grade 4 to this entity. It tipically affect adult patients with a median age of 62 years. Although GBM can arise anywhere in the CNS, it usually affect the supratentorial region; temporal lobe is the most frequent site, followed by parietal lobe, frontal lobe and occipital lobe. Basal ganglia and thalamus also represent common locations; rare sites include brain stem, cerebellum and spinal cord. Hemispheric GBMs usually tend to infiltrate through corpus callosum the contralateral hemisphere (so-called “butterfly GBM”). Leptomeningeal spread is also common.

The obsolete term “glioblastoma multiforme” well suggests the multiple histological aspects showed by the tumor; classically, GBM is a hypercellular lesion, composed of poorly differentiated cells with cytonuclear pleomorphism

and high mitotic index with tendency to display necrosis and/or microvascular proliferation, both representing essential diagnostic clues. Morphology of these tumors varies from patient to patient and also within the same tissue, ranging from forms in which it is still possible to recognize the astrocytic nature of neoplastic cells to undifferentiated ones. GBM may be composed of spindle, epithelioid or round-shaped cells, from large to small in size and may also contain lipidized, giant, granular, small cells or an oligodendroglioma-like component (i.e. round cells with rounded nuclei and clear perinuclear halo). GBM may also show metaplastic changes, such as epithelial squamous metaplasia or areas with glandular and ribbon-like epitelial structures. The mesenchymal differentiation of neoplastic cells may be so marked as simulate a true biphasic tumor with glial and mesenchymal components: in this cases a diagnosis of "gliosarcoma" is encouraged. As previously mentioned, microvascular proliferation and necrosis represent the diagnostic hallmarks of GBM: the former consists of proliferating vessels lined by multilayered and mitotically active/Ki-67 positive endothelial cells, often assuming a tortuous and glomeruloid appearance, the latter may display a palisading morphology consisting of multiple, irregular-shaped, often confluent necrotic foci surrounded by radially oriented neoplastic cells.

IDH wildtype GBM variably express glial cell lineage markers, such as GFAP, OLIG-2, S100 and Vimentin, and EGFR in about 40-50% of cases. IDH R132H is typically negative in these forms. Ki-67 proliferation index may be extremely variable, ranging from cases with a Ki-67 >50%, to cases with low proliferative activity; however, frequent values are 15-20%.

When pathologists face with an adult diffuse gliomas, IDH-wt, lacking necrosis and/or microvascular proliferation, a diagnosis of GBM IDHwt may be rendered based on the presence of at least one of the following molecular features: i) combined chromosome 7p gain and 10q loss, ii) EGFR amplification, iii) TERT promoter mutation.

Chromosome 7p gain combined to 10q loss represents the most common genetic signature of GBM. EGFR amplification is relatively common in GBMs and it is frequently associated with EGFR immunohistochemical overexpression (70-80%). Mutations of PTEN gene occur in 25-35% of IDH-wildtype GBMs, as well as mutations of TP53, far rarer in this entity, in about 25% of cases. CDKN2A deletions and TERT promoter mutations are common in IDH-wildtype GBM. By definition, IDH1 and IDH2 genes are wildtype.

Despite the progress made in treatment of GBM patients, this tumor still remains fatal with the majority of patients dying within 18 months after diagnosis. Presence of MGMT promoter methylation is the strongest indipendent prognostic and predictive factor of therapeutical response: only 35% of patients have methylated MGMT promoter, but about 90% of long-term survivors present this specific molecular trait. Patients who carry MGMT promoter hypermethylation are more sensitive to alkylating chemotherapeutical agents, such as temozolamide. No significant correlation has been found between EGFR amplification and survival.

4. Oligodendroglioma, IDH-mutant and 1p/19q codeleted (WHO grade 2) [44-46]

Oligodendrogliomas are diffusely infiltrating gliomas, first described by Bailey and Cushing in 1926, [47] which by definition harbour mutations in the IDH1 or IDH2 gene, associated with a characteristic complete co-deletion involving the chromosomal arms 1p and 19q. When the mutational status of the IDH1 / IDH2 genes and / or the presence or absence of 1p / 19q codeletion is not evaluable, or provides inconclusive results, WHO recommends the diagnostic use of the term "oligodendroglioma, not otherwise specified (NOS).

WHO grade II oligodendrogliomas are rare neoplasms, accounting for about 1.2% of all brain neoplasms and about 6% of all human gliomas and occurring mainly in adults, with an average age at the diagnosis of about 40 years old; Oligodendrogliomas develop, in most cases, from the white matter of the cerebral hemispheres; the frontal lobes are the most frequent affected site, followed by the temporal, parietal and occipital lobes respectively. Extremely rare localizations are the posterior cranial fossa, the basal ganglia, the brain stem and the spinal cord. Cases of oligodendrogliomas involving more than one cerebral lobe and bilateral growth have also been described. Rarely, they may also have leptomeningeal growth or a diffuse ab initio onset, in the form of gliomatosis cerebri (peculiar growth pattern, involving different portions of the CNS, with no formation of well-defined nodules).

Histologically, WHO grade 2 oligodendroglioma is a moderately cellular neoplasm consisting of a fairly homogeneous population of round-shaped cells, with a rounded central nucleus, and a characteristic perinuclear clear halo of artifactual nature, due to the procedures of formalin fixation and paraffin embedding, that confer to the tumor its characteristic "fried egg" morphology.

Cytologically, neoplastic cells are characterized by hyperdense chromatin with “salt and pepper” aspects. Oligodendrogliomas have a fine and delicate vascularization, consisting of small, thin-walled, branching capillaries, forming the characteristic “chicken-wire” pattern. Presence of numerous intratumoral microcalcifications is a typical, albeit not pathognomonic finding. Some WHO grade II oligodendrogliomas present mucoid and/or microcystic degeneration, intratumoral nodules characterized by increased cellularity and a component of neoplastic cells with astrocytic morphology; however, even in the presence of a morphologically similar to astrocytes cellularity, the evidence of mutation of the IDH1 or IDH2 gene, associated with 1p/19q codelection, allows the diagnosis of IDH-mutated and 1p/19q-codeleted oligodendroglioma. Mitoses are generally absent, but in some cases the presence of an occasional mitosis and/or nuclear atypia is still compatible with the diagnosis of WHO grade II IDH-mutant and 1p/19q-codeleted oligodendroglioma. Increased mitotic activity, necrosis and microvascular proliferation are absent.

Immunohistochemically, most oligodendrogliomas are positively stained with anti-IDH-1 R132H antibody; however, the absence of positivity for this antibody does not rule out the diagnosis, as there are rarer mutations of IDH2 or IDH-1 gene different from R132H portion that are not recognized by the abovementioned antibody; molecular test of gene sequencing must be performed in this setting. Typically, IDH-mutant and 1p/19q-codeleted oligodendrogliomas retain nuclear expression of ATRX and do not exhibit p53 overexpression, differently from the IDH-mutant astrocytoma group. Oligodendroglioma cells show diffuse and strong positivity for OLIG-2, S100 and Microtubule Associated Protein 2 (MAP-2);

MAP-2 in this category of neoplasms shows an intense perinuclear cytoplasmic expression, with no evidence of cytoplasmic processes, more typical of astrocytic neoplastic cells. Vimentin is usually negative in WHO grade 2 oligodendrogliomas, while it can be positive in the higher grade forms. The positivity for GFAP is variable, as this antibody can stain both reactive entrapped astrocytes and neoplastic cells with astrocytic morphology. Ki-67 proliferative index is generally <5%.

In addition to the already mentioned "entity-defining" IDH1/2 mutations and the complete codeletion of chromosomal arms 1p and 19q, most of the grade II IDH-mutant and 1p/19q-codeleted oligodendrogliomas present TERT promoter activating mutations, while, on the contrary, they typically do not harbour ATRX and TP53 mutations. This is consistent with the fact that, in human gliomas, the presence of 1p/19q codelection appears to be mutually exclusive with TP53 gene mutations and TERT promoter mutations never occur alongside those of ATRX gene. WHO grade 2 oligodendrogliomas have a relatively good prognosis, with a mean overall survival of approximately 12 years and a 10-year survival rate of approximately 50%; they tend to locally recur after surgical excision; histological malignant progression after local recurrences is common, although this event occurs more slowly than the astrocytic counterpart of same histological grade.

5. Oligodendroglioma, IDH-mutant and 1p/19q codeleted (WHO grade 3) [45, 47-52]

It is a tumor that harbors by definition mutations of the IDH1 or IDH2 genes, combined to 1p/19q codeletion; anaplastic oligodendroglioma presents at least focal histological findings of anaplasia, including brisk mitotic activity and/or

microvascular proliferation. It preferentially occurs in adults, with a mean age at diagnosis slightly higher than that of grade 2 oligodendrogliomas, of about 50 years. Anaplastic oligodendroglioma generally arises at hemispheric level; the frontal lobes represent the most frequent site of involvement, followed by the temporal ones; other rarer sites (spinal cord, brain stem, etc.) have also been described. It can develop de novo, or as progression from a IDH-mutant and 1p/19q-codeleted WHO grade 2 oligodendroglioma, with an estimated median time to progression of approximately 6-7 years.

WHO grade 3 oligodendrogliomas are highly cellular neoplasms, that diffusely infiltrate the surrounding brain parenchyma and are composed of cells with morphological features resembling those of oligodendroglial cells (rounded shape, round nucleus, clear perinuclear halo); however, features of anaplasia are invariably present: foci of necrosis, microvascular proliferation, nuclear pleomorphism and brisk mitotic activity. Particularly, detection of brisk mitotic activity (defined by some authors as > 6 mitoses/10 HPF) and/or microvascular proliferation are mandatory to render this diagnosis. Branching vascular pattern is also often present in garde 3 oligodendrogliomas, as well as microcalcifications. These tumors can also display an astrocytic morphology, which, if combined to the frequent presence of necrosis and microvascular proliferation, can erroneously lead to the diagnosis of grade 4 glioblastoma. WHO grade 3 anaplastic oligodendrogliomas share the same immunohistochemical finding with their lower grade counterparts; however, Ki-67 proliferative index appears to be higher, generally> 5%, although a specific cut-off point has not been established.

Almost all grade 3 anaplastic oligodendrogliomas have IDH1/2 gene mutations, associated with 1p/19q codeletion; more than 95% of them also harbour mutations of TERT promoter gene and, in 60% of cases, CIC gene mutations. ATRX and TP53 are frequently wildtype. MGMT promoter is frequently hypermethylated, which gives these tumors higher sensitivity to the alkylating agent temozolomide.

WHO grade 3IDH-mutant and 1p/19q-codeleted oligodendrogliomas, despite having a poor prognosis, are characterized by better survival rates than WHO grade 3 astrocytomas, IDH-mutant. Median overall survival is about 3.5 years and the 10-year survival rate is about 39%. Local relapse and progression of the disease is the leading cause of death.

6. Pilocytic astrocytoma (WHO grade 1) [53-57]

Pilocytic astrocytoma (PA) is a slow-growing tumor, genetically characterized by the tandem duplication KIAA1549-BRAF and mutations in genes coding for proteins of the MAPK pathway. WHO assigns to PA a histological grade I. PA commonly arises in children and adolescents with a male predilection, but it can occurs at any age. PA is mainly located in the cerebellum and others midline structures, including optic pathways, brain stem and spinal cord. PA is the most frequent glioma associated to type 1 neurofibromatosis (NF1) and the optic pathways are the most frequent affected site in this clinical setting.

PA is a lowly/moderately cellular lesion with a biphasic pattern, consisting of compacted bipolar cells with Rosenthal fibres and multipolar cells embedded in a loose, sometimes myxoid or microcystic background containing eosinophilic granular bodies. Scattered mitoses, pleomorphic nuclei, foci of necrosis, microvascular proliferation and leptomeningeal spread may be encoutered.

Morphology of PA may be very heterogeneous and tumors with oligodendroglioma-like aspects may also occur. Due to the slow-growing biology of these tumors, sometimes regressive changes, including hyalinized ectatic vessels, haemorrhage with haemosiderin deposits, infarct-like necrosis, calcifications and perivascular lymphocytic infiltration are prominent features.

Immunohistochemical tests tipically reveal strong positivity for GFAP, OLIG-2 and S100; synaptophysin may be weakly positive and should not be interpreted as evidence of glioneuronal neoplasm. P53 is absent or weakly positive; IDH1 R132H is tipically negative. A small subset of PAs shows an immunohistochemical positivity for BRAFV600E. Ki-67 index is tipically very low.

A tandem duplication of 7q34 in BRAF gene, resulting in a fusion gene between KIAA1549 and BRAF, is the most typical genetic change of PAs (present in >70% of patients). In addition to KIAA1549-BRAF fusion (present in almost all cases located in the cerebellum), all PAs present alterations in genes involved in the MAPK pathway, including NF1 and BRAFV600E mutations (more common in supratentorial neoplasms). IDH-1/2, TP53 and ATRX are tipically wild-type.

Prognosis of PA is tipically favourable with 10 years OS rate >95% after surgery. Rarely, PA can recur and progress in forms with anaplastic changes; however, the concept of anaplastic transformation of AP and the histological parameters of such anaplastic changes have not yet been well clarified, being limited only to cases recurred after surgery, or undergone prior irradiation therapy.

7. Ependymoma [58-65]

Ependymomas are circumscribed gliomas composed of small cells with rounded nuclei arranged in perivascular pseudorosettes and ependymal rosettes. They can affect almost all sites of CNS; however, ependymomas of children preferentially occur intracranially (posterior fossa is the preferred site), whereas in adults they are most frequently spinal tumors. WHO classification recognizes multiple clinico-pathological entities by assigning them different histological grades. Briefly, subependymomas (WHO grade 1) are mostly located to the fourth or the lateral ventricles. Myxopapillary ependymomas (WHO grade 2), preferentially occurs in the lower spinal cord (conus medullaris, cauda equina and filum terminale). The category of classic ependymomas (WHO grade 2) comprise different histopathological variants, including papillary, clear cell, or tanycytic ependymoma. Anaplastic ependymomas (WHO grade 3) are hypercellular neoplasms with high mitotic count, necrosis, and microvascular proliferation. In 2016 WHO introduced a novel molecularly defined subset of ependymomas, characterized by RELA fusion gene ("Ependymoma, RELA fusion-positive"). defines a distinct category of supratentorial WHO grade 2 and grade 3 ependymomas in children and young adults. Immunohistochemical staining for L1CAM or p65 can be used as a readily usable surrogate marker for the presence of RELA fusion. In general, ependymomas are circumscribed gliomas composed of uniformely round cells with round to oval nuclei, forming perivascular anucleate areas (perivascular pseudorosettes) and in a minority of cases true ependymal rosettes. Cellularity and nuclear atypia greatly vary according to the histological grade and the specific ependymoma subtype.

Immunohistochemically, ependimomas are uniformely characterized by positive staining for GFAP, S100 and Vimentin; whereas OLIG-2 and Synaptophysin are generally negative. A useful diagnostic clue is that ependymoma is the only glioma showing positivity for GFAP combined to absence of OLIG-2 staining. In addition, most ependymomas show a typical perinuclear dot-like or ring-like cytoplasmic positivity for EMA. Cytokeratins may be focally positive. Strong immunoreactivity for L1CAM and p65 is tipically found in ependymomas, RELA fusion-positive. Children with ependymoma have a worse prognosis than adults and the anatomical localization (intracranial vs spinal) probably explain these differences. Gross total resection is significantly associated with better outcome in both categories of patients.

8. CircSMARCA5-SRSF1 molecular axis

Circular RNAs (circRNAs) are a recently found wide group of RNAs with biological functions not yet fully clarified [66,67]. However, the expression of several circRNAs has been found deregulated in several human disease from neoplastic to degenerative ones, suggesting an active role of circRNAs in their pathogenesis [66,67]. Recently, a circular RNA (circSMARCA5) that has been found downregulated in GBM biopsies with respect to normal brain parenchyma, as a decoy for the oncogenic serine and arginine rich splicing factor 1 (SRSF1), has been characterized [68,69]. It has been also demonstrated that modulation of circSMARCA5 expression influences the splicing pattern of vascular endothelial growth factor A (VEGFA) in the cell line U87MG, used as GBM *in vitro* model [68,69]. SRSF1 has been recently characterized as functionally involved in

gliomagenesis: in particular, this protein that normally shuttles between the nucleus (where, once phosphorilated, accumulates in the speakles contributing to the assembly of the spliceosome) and the cytoplasm (where it interacts with other proteins) is upregulated in GBM and contributes in the aberrant splicing of a plethora of target pre-mRNAs [68,69]. Recently, Zhou et al [70] found that SRSF1 is increased both in glioma tissues and cell lines and its increased immunohistochemical expression was positively correlated with histological grade (grade 2 diffuse astrocytoma vs grade 3 anaplastic astrocytoma vs grade 4 GBM) and Ki-67 index and predicted poorer prognosis in GBM patients subset.

9. Aim of the study

The aim of this research is to study both at immunohistochemical and molecular level the selective activation of CircSMARCA5-SRSF1 molecular axis in a cohort of GBM biopsies and correlate these findings with histological and molecular features and clinical outcome data. A further interesting perspective of the study is to test the immunohistochemical expression of SRSF1 on a cohort of non-astrocytic adult gliomas, that have to be frequently considered in the differential diagnosis of astrocytic tumors, including oligodendrogliomas, ependymomas, pilocytic astrocytoma, subependymal giant cell astrocytoma and pleomorphic xanthoastrocytoma in order to evaluate the potential diagnostic utility of this protein in the neuropathological practice.

10. Material and methods

Cases have been retrieved from the pathology files of the Section of Anatomic Pathology, Department of Medical, Surgical, and Advanced Technologies "G.F. Ingrassia", University of Catania. University of Catania. Only confirmed cases, both histologically and molecularly of IDH-wild type GBM (*n* = 42), IDH-mutant and 1p/19q co-deleted oligodendroglioma (*n* = 21), ependymoma (*n* = 15), pilocytic astrocytoma (PA) (*n* = 15), sub-ependymal giant cell astrocytoma (SEGA) (*n* = 5) and pleomorphic xanthoastrocytoma (PXA) (*n* = 4), diagnosed during the period between 2015 and 2021, have been included in the study. Clinical data were obtained from the original pathological reports. Overall survival (OS) times were available only for 28/42 GBM cases. Regarding the GBM cohort, non neoplastic brain tissue was also excised during surgery, when possible, from a non-eloquent brain region, adjacent to the neoplastic area and negative to 5-aminolevulinic acid (5-ALA) fluorescence: this non neoplastic tissue has been used as control tissue after pathological examination confirmed absence of infiltration of glioma cells (*n*=20). Molecular tests, through quantitative real time polymerase chain reaction (qRT-PCR) and next-generation sequencing (NGS), have been retrospectively performed on each case., in order to precisely define the "molecular asset" of the each glioma examined (in terms of IDH1/IDH2, ATRX and TP53 mutations, and MGMT promoter methylation status) and characterize circSMARCA5 and SRSF1 expression. A standard approach based on immunohistochemistry (IHC) and NGS has been applied to retrospectively reclassify each case according to 2021 WHO classification: each tumor section underwent IHC for IDH1 (R132H), ATRX, p53, EGFR and SFRS1,

followed by targeted NGS to confirm the immunohistochemical results. CircSMARCA5 and SRSF1 levels have been investigated by qRT-PCR both on GBM and unaffected brain samples.

Each tumor section has been tested for immunohistochemical analyses using the streptavidin/biotin-based system for immunoperoxidase. Briefly, after appropriate deparaffinization and pre-treatments, sections have been incubated with mouse monoclonal anti-SRSF1 (clone sc-33652) antibody, diluted 1:50 in PBS, mouse monoclonal anti-IDH1 R132H (clone H09) antibody, diluted 1:100 in PBS, mouse monoclonal anti-ATRX (clone AX1) antibody, diluted 1:100 in PBS, mouse monoclonal anti-EGFR (clone H11) antibody, diluted 1:200 in PBS, and mouse monoclonal anti-p53 (clone DO-7) antibody, diluted 1:50 in PBS. For molecular studies, RNA has been purified from formalin fixed and paraffin embedded sections adjacent to those used for immunohistochemical studies, according to RecoverAll™ Total Nucleic Acid Isolation Kit (LifeTechnologies™)'s protocol. PCR reaction has been performed by using one-step Power SYBR® Green RNA-to-CT™ 1-Step Kit (LifeTechnologies™). The following amplification conditions has been used: template denaturation and polymerase activation at 95 °C for 30 s, followed by 40 cycles of denaturation at 95 °C for 15 s, annealing at 60 °C for 30 s, and extension at 72 °C for 30 s. Three technical replicates have been conducted in each PCR reaction. Finally, clinical data from each GBM patient in terms of age, sex, OS and progression free survival (PFS) have been collected, whereas the only clinical parameters available for other non-GBM gliomas enrolled in the study were age and sex.

10.1 Immunohistochemical evaluation of SRSF1

Immunohistochemical sections have been evaluated without information on clinical data. The presence of brown chromogen in the nucleus of cells has been interpreted as positive SRSF1 staining. No cytoplasmic staining has been observed in any case. Normal gallbladder tissue has been used as external positive control to check the validity of the immunoreaction. Evaluation of the different staining pattern of SRSF1 has been performed, as previously described [70,71]. Intensity of staining (IS) has been graded on a 0-3 scale (0= absent staining , 1= weak staining, 2= moderate staining, 3=strong staining). Five categories (0-4) of percentage of SRSF1 immunopositive cells (Extent Score, ES) have been identified: <5%; 5–30%; 31–50%; 51–75%; >75%. IS has been multiplied by ES to obtain the immunoreactivity score (IRS); low (L-IRS) and high (H-IRS) expression of SRSF1 have been defined as IRS < 6 and IRS ≥ 6, respectively.

11. Results

11.1 Clinico-pathological and molecular features of glioma cohort

Among the 42 GBM cases, 19 patients (45%) were males and 23 (55%) were females (mean age: 63 years). As regards the specific anatomic site, 23 GBMs (55%) were located at the temporal lobe, 10 (24%) at the parietal lobe and 9 (21%) at the frontal lobe, three of which presented contralateral spread. All 42 GBM cases were histologically and molecularly classified as WHO grade IV IDH-wild type; neither IDH1/2 mutations nor ATRX mutations were identified at the immunohistochemical and molecular levels; no evidence of 1p/19q co-deletion was found; p53 immunohistochemical overexpression was found in only seven

cases (17%), but no TP53 mutation was molecularly identified. O^6-methylguanine DNA methyltransferase (MGMT) promoter were not hypermethylated in all cases. The mean OS of the 28 GBM cases for which follow-up data were available was 17 months. Among the 21 oligodendroglioma patients, 12 (57%) were males and nine (43%) were females (mean age: 59 years). All oligodendrogliomas were located supratentorially, 8/21 (38%) at the temporal lobe, 7/21 (33%) at the parietal lobe and the remaining 6 (29%) at the frontal lobe. Histologically, 15/21 (71%) were diagnosed as WHO grade II oligodendroglioma and 6/21 (29%) as grade III anaplastic oligodendroglioma. All oligodendrogliomas included in the study presented IDH-1 (R132H) mutations, confirmed both immunohistochemically and molecularly. The 1p/19q co-deletion was found in 21/21 cases (100%). Of the individuals affected by ependymoma, 9/15 patients (60%) were males and 6/15 (40%) were females (mean age: 56 years). A total of 11/15 (74%) ependimomas were localized supratentorially, 2/15 (13%) in the posterior fossa and 2/15 (13%) in the spinal cord. Histologically, 14/15(93%) were diagnosed as WHO grade II classic ependymomas, 1/15 (7%) as WHO grade I myxopapillary ependymoma. All ependymomas were positively stained with GFAP and at least focally with EMA (dot-like/ring-like staining). OLIG-2 was negative in 13/15 cases (87%). IDH1/2, TP53, ATRX genes were wild type. No 1p/19q co-deletion was found in any case. Among the PA patients, 11/15 (73%) were males and 4/15 (27%) were females, with a mean age at diagnosis of 23 years. 14/15 tumors (93%) were located at the cerebellum and 1/15 (7%) at the spinal cord. Immunohistochemical and molecular profiles of these tumors were relatively homogenous, showing diffuse positivity for GFAP and OLIG-2, focal

expression of synapthophysin and absence of IDH 1/2, ATRX, TP53 mutations and 1p/19q co-deletion. All PAs included in the study showed a molecularly proven KIAA1549-BRAF fusion. Of the affected by SEGA, 3/5 patients (60%) were males and 2/5 (40%) were females (mean age: 21 years); all tumors (5/5) were located in the wall of the lateral ventricles and were associated to tuberous sclerosis syndrome. Immunohistochemically, all SEGAs were diffusely stained with GFAP, s-100 and SOX-2; focal positivity for synaptophysin was seen in 1/5 cases. Neither IDH 1/2, ATRX, TP53, BRAFV600E mutations, nor 1p/19q co-deletions were found. Finally, among the PXA patients, 3/4 (75%) were females and 1/4 (25%) male, with a mean age at the diagnosis of 26 years; 3/4 PXAs (75%) were located at the temporal lobe and 1/4 (25%) at the parietal lobe. Histologically, three cases (75%) were diagnosed as WHO grade II PXA and one case (25%) as WHO grade III anaplastic PXA; neoplastic cells exhibited an immunopositivity for GFAP in 4/4 cases and for synaptophysin in 1/4 cases; extravascular positivity for CD34 was observed in 3/4 cases. BRAFV600E mutations were molecularly found in 2/4 PXAs.

11.2 SRSF1 immunohistochemical expression in GBMs, normal brain tissue and other gliomas.

Among the 42 GBMs, 34/42 (81%) cases showed high immunohistochemical expression of SRSF1 (IRS ≥ 6) (**Figure 1**), whereas only in 8/42 (19%) low levels of immunohistochemical expression of SRSF1 (IRS < 6) were found. High SRSF1 levels (IRS ≥ 6) were found in 15/21 cases (71%) of oligodendrogliomas (**Figure 2**), whereas only 6/21 (29%) showed low expression (IRS < 6); all cases

(6/6) of grade III anaplastic oligodendrogliomas had an IRS value ≥ 6. 2/15 (13%), ependymomas showed low SRSF1 levels (IRS < 6) and in the remaining 13/15 cases (87%), SRSF1 immunoexpression was completely absent (IRS = 0) (**Figure 3**). Similarly, low SRSF1 expression levels (IRS < 6) were found in 5/15 (33%) PAs (**Figure 4**) and in 10/15 cases (67%) no immunostaining (IRS = 0) was detected. Among the five SEGAs, 4/5 cases (80%) exhibited high SRSF1 immunoexpression (IRS ≥ 6) (**Figure 5**A,B), while a low level of SRSF1 immunoexpression was found in only one case (20%). Finally, 3/4 cases (75%) of PXA showed IRS values ≥ 6 (**Figure 5**C,D) and the remaining case (25%) had an IRS value < 6.

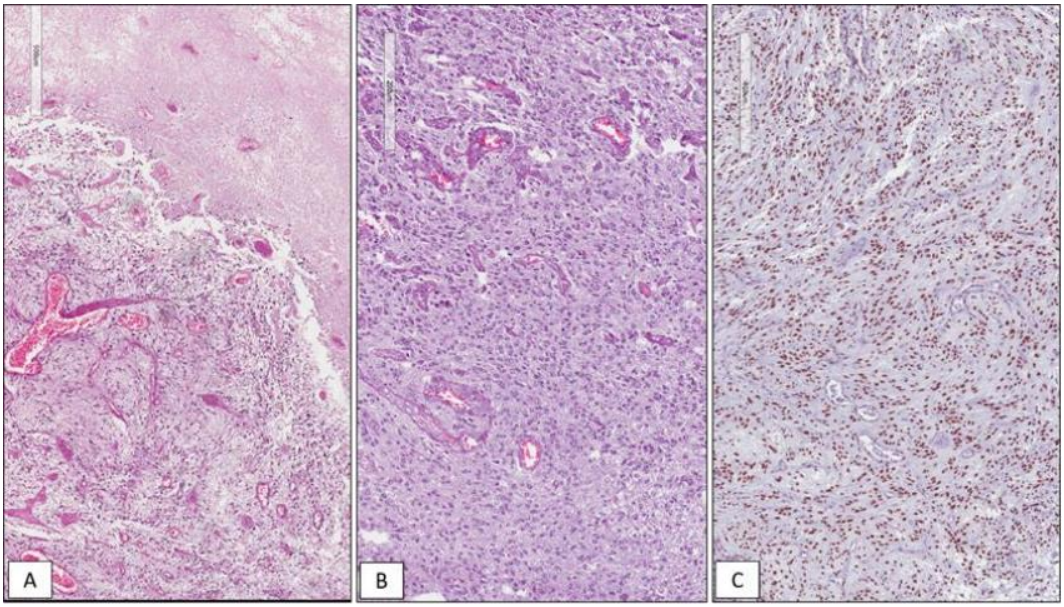

Figure 1. WHO grade 4 IDH wild type glioblastoma. Histopathological examination showing a hypercellular glial tumor with extensive necrosis (**A**) and microvascular proliferation (**B**); high immunohistochemical nuclear expression of SRSF1 in a GBM tissue sample (**C**) (hematoxylin and eosin(**A**,**B**) and immunoperoxidase (**C**) staining; original magnifications 50×, 100× and 100×).

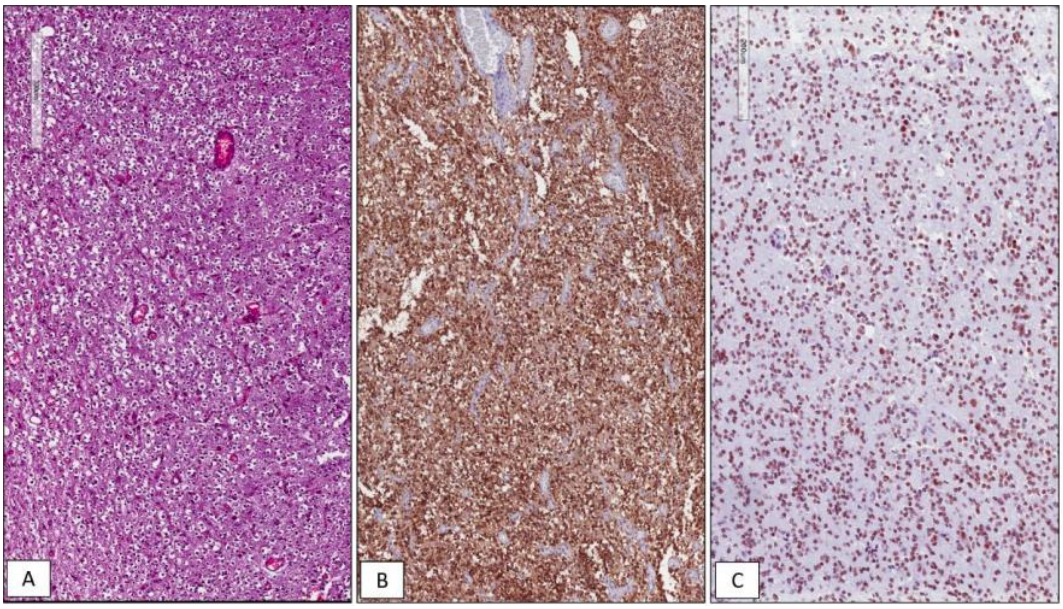

Figure 2. WHO grade 2 IDH mutant and 1p/19q co-deleted oligodendroglioma. Histopathological examination showing a moderately cellular glial tumor, composed of bland-looking round cells with a perinuclear clear halo with no evidence of necrosis and/or vascular proliferation (**A**); immunohistochemical positivity for IDH1 R132H reveals the presence of an IDH-1 gene mutation (**B**); high immunohistochemical nuclear expression of SRSF1 in WHO grade 2 oligodendroglioma (**C**) (hematoxylin and eosin (**A**) and immunoperoxidase (**B**,**C**) staining; original magnifications 100×, 100× and 100×).

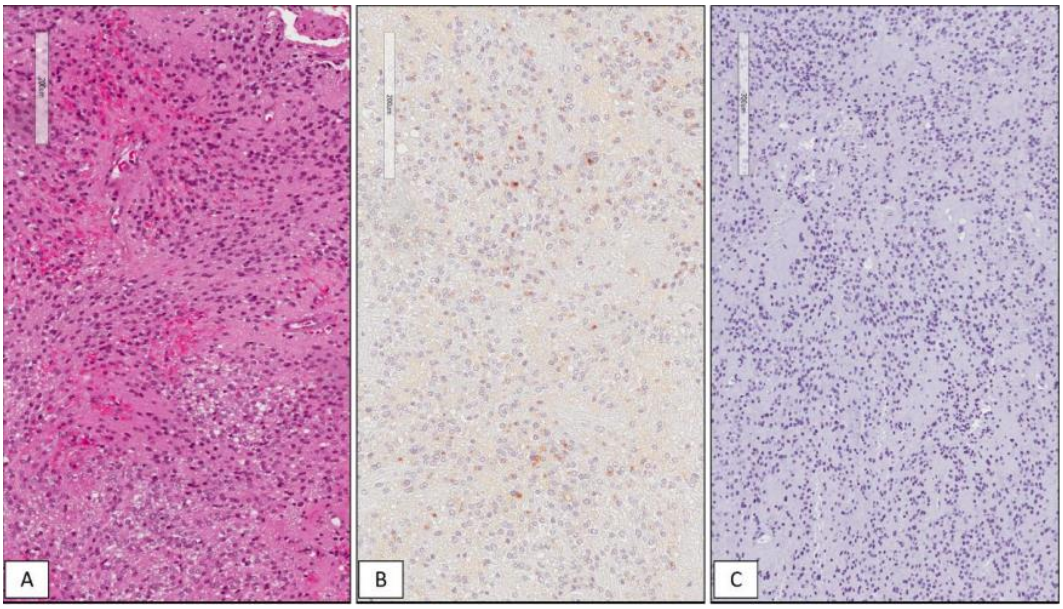

Figure 3. WHO grade 2 classic ependymoma. Histopathological examination showing a moderately cellular lesion, composed of small cells with rounded nuclei arranged in perivascular pseudorosettes with no evidence of anaplastic features (**A**); perinuclear "dot-like" staining for EMA highly suggestive for a diagnosis of ependymoma (**B**); absence of immunohistochemical expression of SRSF1 in WHO grade 2 classic ependymoma (**C**) (hematoxylin and eosin (**A**) and immunoperoxidase (**B**,**C**) staining; original magnifications 100×, 100× and 100×).

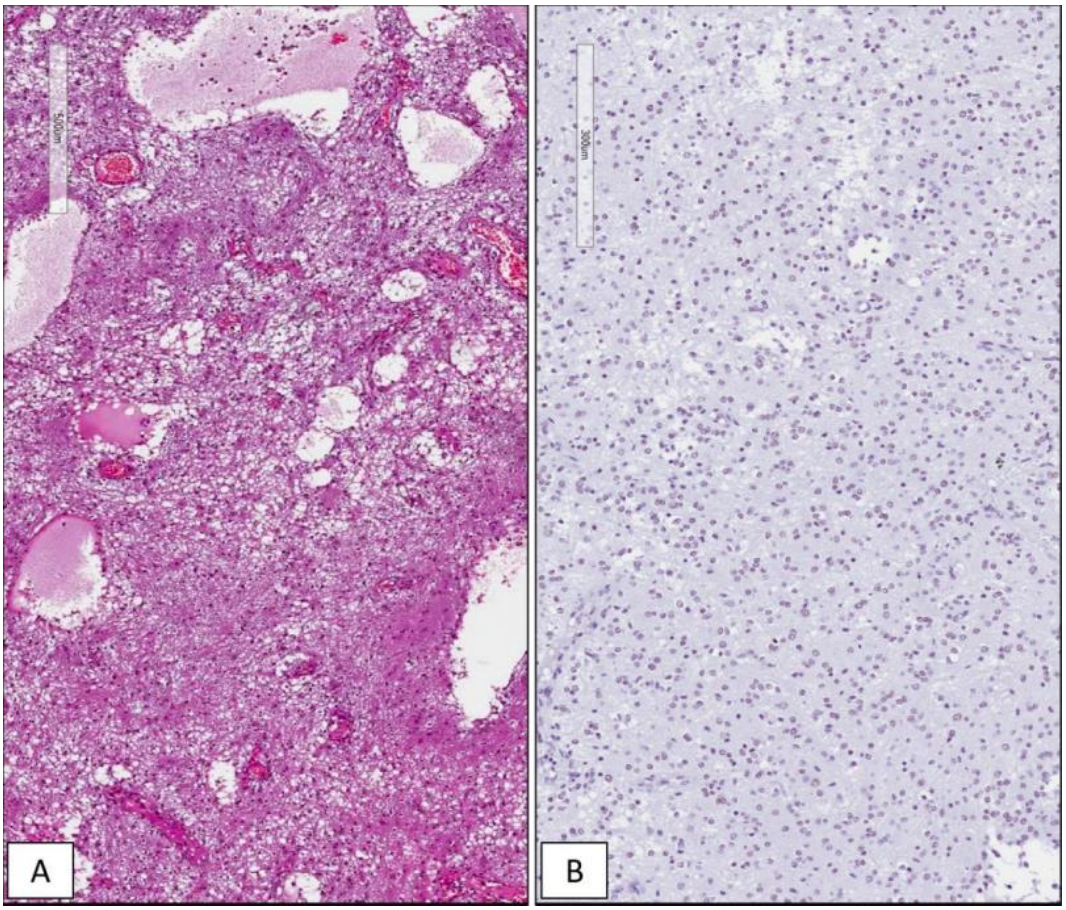

Figure 4. WHO grade 1 pilocytic astrocytoma. Histopathological examination showing the typical biphasic appearance consisting of compacted bipolar cells with Rosenthal fibers and multipolar cells embedded in a loose, myxoid and/or microcystic background (**A**); weak and focal nuclear immunohistochemical expression of SRSF1 in WHO grade 1 pilocytic astrocytoma (**B**) (hematoxylin and eosin (**A**) and immunoperoxidase (**B**) staining; original magnifications 100×).

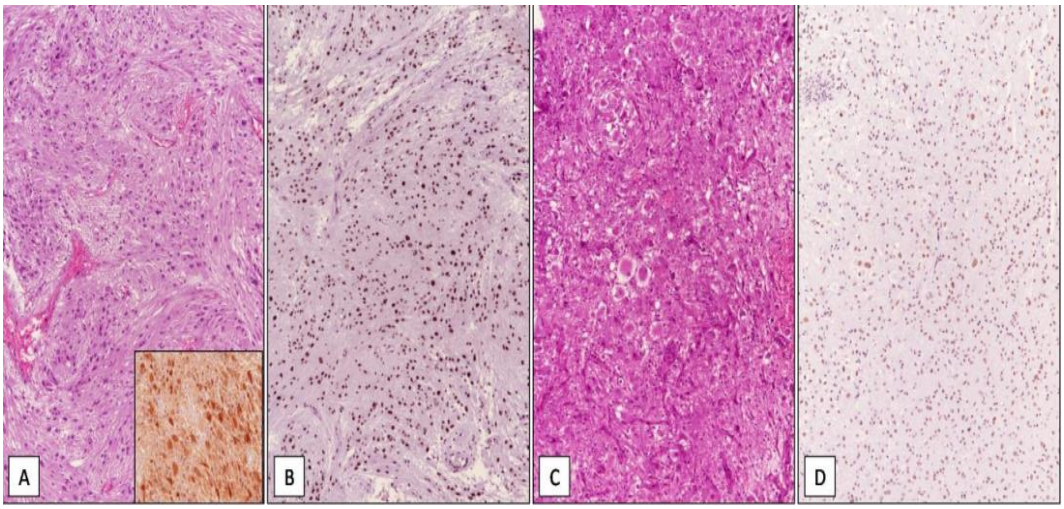

Figure 5. Sub-ependymal giant cell astrocytoma and pleomorphic xanthoastrocytoma. (**A**) Histopathological examination of sub-ependymal giant cell astrocytoma showing large polygonal to elongated cells with ganglioid/gemystocytic-like morphology and abundant eosinophilic cytoplasm; neoplastic cells typically exhibiting strong immunoreactivity for s-100 (insert); (**B**) strong and diffuse immunohistochemical expression of SRSF1 in sub-ependymal giant cell astrocytoma. (**C**) Histopathological examination of WHO grade II pleomorphic xanthoastrocytoma showing pleomorphic mono and multinucleated cells with focal cytoplasmic xanthomatous changes; (**D**) neoplastic cells were strongly and diffusely stained with SRSF1 (hematoxylin and eosin (**A**,**C**) and immunoperoxidase (**B**,**D**) staining; original magnifications 100×).

11.3 Correlation between circSMARCA5 expression, VEGFA pro- (Iso8a) and anti angiogenetic (Isp8b) isoform ratio and immunohistochemical expression of SRSF1

SRSF1 immunohistochemical expression appeared to be significantly upregulated in GBM biopsies, compared to normal control brain tissue (NORM) (p-value =

0.01867, Student's t-test, n_{GBM} = 42; n_{NORM} = 20) (**Figure 6**), confirming the trend reported in literature. SRSF1 positivity was exclusively found within the nuclei.

Figure 6. SRSF1 immunohistochemical expression.

A negative correlation at the limit of statistical significance between circSMARCA5 and SRSF1 expression on the entire cohort studied (n_{GBM} = 42; n_{NORM} = 20) was found (r-value = -0.26716, p-value = 0.05554, Spearman's correlation test). Analyzing the subset of patients for which it was possible to obtain real-time PCR data also for the single mRNA isoforms (pro- and anti-angiogenic) of VEGFA, the negative correlation trend was maintained but statistical significance was lower, probably due to the reduction in the number of samples analyzed (r-value = -0.2371, p-value = 0.1770, Spearman's correlation test, n_{GBM} = 28; n_{NORM} = 6) (**Figure 7**). As expected, based on the positive control played by the splicing factor SRSF1 on the ratio between the expression of VEGFA proangiogenic isoform (Iso8a) and antiangiogenic one (Iso8b), a positive

correlation was observed between the SRSF1 expression and the Iso8a / Iso8b ratio (r-value = 0.2867, p-value = 0.1001, Spearman's correlation test, nGBM = 28; nNORM = 6). Likewise, the absence of statistical significance was probably due to the low number of cases analyzed.

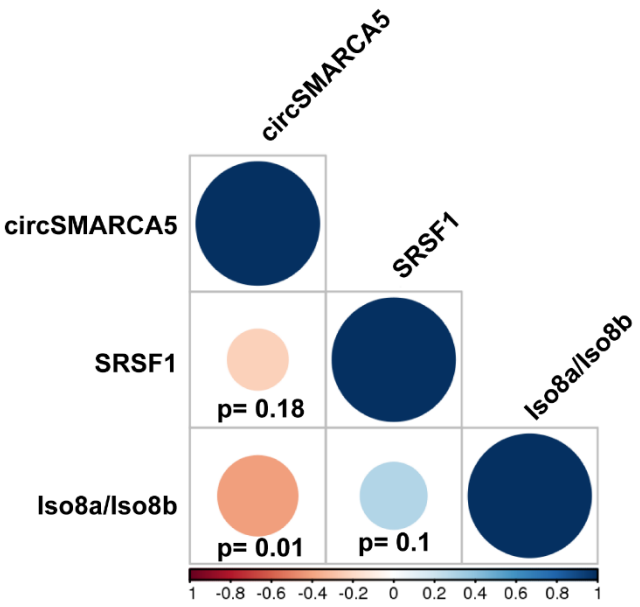

Figure 7. Correlations between circSMARCA5 expression, VEGFA pro- (Iso8a) and anti angiogenetic (Isp8b) isoform ratio and SRSF1. Blue values indicate a positive correlation; red values a negative one. Color intensity and the diameter of the circles are proportional to the correlation coefficients. (Spearman correlation test, n_{GBM} = 28; n_{NORM} = 6).

11.4 Correlation between Immunohistochemical Expression of SRSF1 and Prognosis

Analysis of Kaplan–Meier survival curve showed that GBM patients with high immunoexpression of SRSF1 had lower OS times than the GBM group with low immunoexpression of this protein: median OS of patients with high immunoexpression of SRSF1 was 18.0 months (IQR 12.0–23.0), while patients

with low SRSF1 levels exhibited median OS of 23.0 months (IQR 18.0–24.0) (p = 0.18). **Figure 8** shows Kaplan–Meier survival estimates for the two groups.

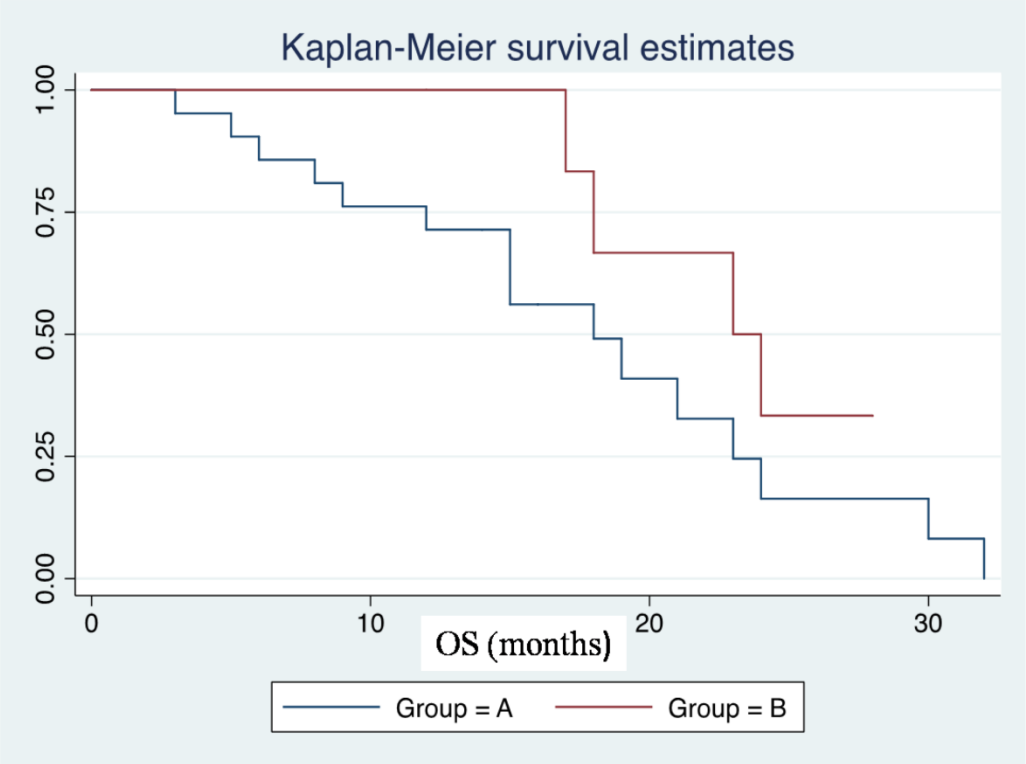

Figure 8. Group A (n = 21): patients affected by GBM with IRS_{SRSF1} values ≥ 6; Group B (n = 7): Patients affected by GBM with IRS_{SRSF1} values < 6.3.4.

12. Discussion

CircRNAs represents a wide subgroup of RNAs whose biology and active role in the cellular metabolic "life" still remain largely unknown [68-68]. To date, in scientific literature there are numerous papers that describe how some specific circRNAs are effectively deregulated in several human degenerative and neoplastic diseases [66-69]. It is also known that splicing is the mechanism

through which these RNAs originate [66-69]. It has been described that multiple circRNAs are highly expressed in human brain normal and neoplastic tissue and oncogenetic processes, including cellular differentiation and epithelial-to-mesenchymal transition, regulate their differential expression [66-69]. Barbagallo et al [68,69] investigated the expression of 12 different types of circRNAs in both human unaffected brain parenchyma and CNS glial tumors and found that circSMARCA5 represents the best example of downregulated circRNA in WHO grade 4 GBM IDHwt specimens compared to normal cerebral tissue instead; particularly, circSMARCA5 seems to act as a tumor-suppressor RNA, negatively regulating cell migration through the RNA binding protein SRSF1, that in normal conditions acts as an oncoprotein with positive regulatory role on cell migration [68-69]. As a consequence, SRSF1 was found upregulated in GBM biopsies compared to normal brain [68-69]. It has been also demonstrated that SRSF1 is involved in the splicing of VEGFA. The VEGFA pre-mRNA splicing mechanism may alternatively generate both pro-angiogenic and anti-angiogenic isoforms; it has been hypothesized that the downregulation of circSMARCA5, through the concomitant upregulation of SRSF1, lead to a switch of the proangiogenic-antiangiogenic ratio of VEGFA, resulting in an angiogenic stimulation on GBM tissue [68,69]. The fact that patients affected by GBM with circSMARCA5 downregulation had poorer prognosis than those with higher circSMARCA5 expression further supported these findings [68,69].

In this study we tested the immunohistochemical expression of SRSF1 in the same cohort of patients studied by Barbagallo et al [68,69]; we found that SRSF1 immunohistochemical expression was significantly increased in GBM biopsies,

with respect to non neoplastic cerebral tissue used as normal control. Moreover, as expected we found an inverse correlation between circSMARCA5 and SRSF1 expression and a positive one between the SRSF1 expression and the VEGFA Iso8a / Iso8b isoform ratio. Survival analysis confirmed that GBM patients whose biopsies had higher SRSF1 IRS values had a lower survival rate than the group with lower SRSF1 IRS values.

A further potential application field of this study is use of SRSF1 immunoexpression in the diagnostic approach to adult gliomas. To date there are no immunomarkers capable of specifically differentiating astrocytic diffuse gliomas from oligodendroglial, ependymal and pilocytic tumors. All the markers currently used in the histological diagnostic practice, including GFAP, OLIG-2, Vimentin and S100, are broad glial lineage markers, not useful in distinguishing between diffuse astrocytomas, oligodendrogliomas, ependymomas or adult pilocytic astrocytomas. Apart from OLIG-2 which is usually negative in ependymomas [70-72], the other above-mentioned markers are consistently expressed in all gliomas. This is especially true in the broad category of IDH-wildtype gliomas, in which the absence of IDH1-2 mutations makes the differential diagnosis even more though since based on morphology alone. It has been previously demonstrated that SRSF1 is consistently immunohistochemically expressed in adult diffuse astrocytomas and its immunoexpression positively correlates with increased histological grading [70]. In this study we tested the immunohistochemical expression of SRSF1 in a cohort of patients affected by glial neoplasms different from astrocytomas/glioblastomas, including 21 oligodendrogliomas, 15 ependymomas, 15 Pas, 5 SEGAs and 4 PXAs. We found

high SRSF1 expression levels in most oligodendrogliomas (15/21; 71%), SEGAs (4/5; 80%) and PXAs (3/4; 75%), an absence of SRSF1 staining in 13/15 (87%) ependymomas and in 10/15 (67%) PAs; the remaining ependymoma (2/15) and PA (2/15) cases showed weak SRSF1 expression.

Despite being aware of the relatively low number of cases examined, these results would suggest a strong diagnostic utility of SRSF1 protein in distinguishing adult diffuse astrocytomas from ependymomas and PAs (especially in tumors occurred in adults and in non-cerebellar localization). Regarding the diagnosis of oligodendroglioma, a potential application of SRSF1 would be in the distinction between oligodendrogliomas with astrocytic-like morphology and grade II and III adult astrocytomas, that may present a oligodendroglioma-like cellular component, as SRSF1 appears to be more diffusely expressed in former and less expressed in the latter [73].

13. References

1. Davis ME. Epidemiology and Overview of Gliomas. Semin Oncol Nurs. 2018 Dec;34(5):420-429.
1. Molinaro AM, Taylor JW, Wiencke JK, Wrensch MR. Genetic and molecular epidemiology of adult diffuse glioma. Nat Rev Neurol. 2019 Jul;15(7):405-417.
2. Ostrom QT, Gittleman H, Liao P, Vecchione-Koval T, Wolinsky Y, Kruchko C, Barnholtz-Sloan JS. CBTRUS Statistical Report: Primary brain and other central nervous system tumors diagnosed in the United States in 2010-2014. Neuro Oncol. 2017 Nov 6;19(suppl_5):v1-v88.

3. Ostrom QT, Cioffi G, Gittleman H, Patil N, Waite K, Kruchko C, Barnholtz-Sloan JS. CBTRUS Statistical Report: Primary Brain and Other Central Nervous System Tumors Diagnosed in the United States in 2012-2016. Neuro Oncol. 2019 Nov 1;21(Suppl 5):v1-v100.
4. Ostrom QT, Patil N, Cioffi G, Waite K, Kruchko C, Barnholtz-Sloan JS. CBTRUS Statistical Report: Primary Brain and Other Central Nervous System Tumors Diagnosed in the United States in 2013-2017. Neuro Oncol. 2020 Oct 30;22(Supplement_1):iv1-iv96.
5. McNeillKA. Epidemiology of brain tumors. Neurol Clin. 2016; 34:981–998.
6. Louis DN, Perry A, Reifenberger G, von Deimling A, Figarella-Branger D, Cavenee WK, Ohgaki H, Wiestler OD, Kleihues P, Ellison DW. The 2016 World Health Organization Classification of Tumors of the Central Nervous System: a summary. Acta Neuropathol. 2016 Jun;131(6):803-20.
7. Louis DN, Perry A, Wesseling P, Brat DJ, Cree IA, Figarella-Branger D, Hawkins C, Ng HK, Pfister SM, Reifenberger G, Soffietti R, von Deimling A, Ellison DW. The 2021 WHO Classification of Tumors of the Central Nervous System: a summary. Neuro Oncol. 2021 Aug 2;23(8):1231-1251. doi: 10.1093/neuonc/noab106. PMID: 34185076; PMCID: PMC8328013.
8. Ammendola S, Broggi G, Barresi V. IDH-mutant diffuse gliomas: tips and tricks in the era of genomic tumor classification. Histol Histopathol. 2023 Jul;38(7):739-753. doi: 10.14670/HH-18-582. Epub 2023 Jan 9. PMID: 36651583.

9. Hoshide R, Jandial R. 2016 World Health Organization Classification of Central Nervous System Tumors: An Era of Molecular Biology. World Neurosurg. 2016 Oct;94:561-562.
10. Reuss DE, Sahm F, Schrimpf D, Wiestler B, Capper D, Koelsche C, Schweizer L, Korshunov A, Jones DT, Hovestadt V, Mittelbronn M, Schittenhelm J, Herold-Mende C, Unterberg A, Platten M, Weller M, Wick W, Pfister SM, von Deimling A. ATRX and IDH1-R132H immunohistochemistry with subsequent copy number analysis and IDH sequencing as a basis for an "integrated" diagnostic approach for adult astrocytoma, oligodendroglioma and glioblastoma. Acta Neuropathol. 2015 Jan;129(1):133-46.
11. Mirchia K, Richardson TE. Beyond IDH-Mutation: Emerging Molecular Diagnostic and Prognostic Features in Adult Diffuse Gliomas. Cancers (Basel). 2020;12:E1817.
12. Brat DJ, Aldape K, Colman H, et al. cIMPACT-NOW update 3: recommended diagnostic criteria for "Diffuse astrocytic glioma, IDH-wildtype, with molecular features of glioblastoma, WHO grade IV". Acta Neuropathol. 2018;136:805-810.
13. Liu J, Zhang X, Yan X, Sun M, Fan Y, Huang Y. Significance of TERT and ATRX mutations in glioma. Oncol Lett. 2019 Jan;17(1):95-102.
14. Bai HX, Zou Y, Lee AM, Tang X, Zhang P, Yang L. Does morphological assessment have a role in classifying oligoastrocytoma as 'oligodendroglial' versus 'astrocytic'? Histopathology. 2016 Jun;68(7):1114-5. doi: 10.1111/his.12891.

15. Turkalp Z, Karamchandani J, Das S. IDH mutation in glioma: new insights and promises for the future. JAMA Neurol. 2014 Oct;71(10):1319-25.
16. Dang L, White DW, Gross S, Bennett BD, Bittinger MA, Driggers EM, Fantin VR, Jang HG, Jin S, Keenan MC, Marks KM, Prins RM, Ward PS, Yen KE, Liau LM, Rabinowitz JD, Cantley LC, Thompson CB, Vander Heiden MG, Su SM. Cancer-associated IDH1 mutations produce 2-hydroxyglutarate. Nature. 2009 Dec 10;462(7274):739-44.
17. Lu C, Ward PS, Kapoor GS, Rohle D, Turcan S, Abdel-Wahab O, Edwards CR, Khanin R, Figueroa ME, Melnick A, Wellen KE, O'Rourke DM, Berger SL, Chan TA, Levine RL, Mellinghoff IK, Thompson CB. IDH mutation impairs histone demethylation and results in a block to cell differentiation. Nature. 2012 Feb 15;483(7390):474-8.
18. Turcan S, Rohle D, Goenka A, Walsh LA, Fang F, Yilmaz E, Campos C, Fabius AW, Lu C, Ward PS, Thompson CB, Kaufman A, Guryanova O, Levine R, Heguy A, Viale A, Morris LG, Huse JT, Mellinghoff IK, Chan TA. IDH1 mutation is sufficient to establish the glioma hypermethylator phenotype. Nature. 2012 Feb 15;483(7390):479-83.
19. Liu J, Zhang X, Yan X, Sun M, Fan Y, Huang Y. Significance of TERT and ATRX mutations in glioma. Oncol Lett. 2019 Jan;17(1):95-102.
20. Karsy M, Guan J, Cohen AL, Jensen RL, Colman H. New Molecular Considerations for Glioma: IDH, ATRX, BRAF, TERT, H3 K27M. Curr Neurol Neurosci Rep. 2017 Feb;17(2):19.
21. Nandakumar P, Mansouri A, Das S. The Role of ATRX in Glioma Biology. Front Oncol. 2017 Sep 29;7:236.

22. Fogli A, Dematteï MV, Corset L, Vaurs-Barrière C, Chautard E, Biau J, Kémény JL, Godfraind C, Pereira B, Khalil T, Grandin N, Arnaud P, Charbonneau M, Verrelle P. Detection of the alternative lengthening of telomeres pathway in malignant gliomas for improved molecular diagnosis. J Neurooncol. 2017 Nov;135(2):381-390.
23. Conte D, Huh M, Goodall E, Delorme M, Parks RJ, Picketts DJ. Loss of Atrx sensitizes cells to DNA damaging agents through p53-mediated death pathways. PLoS One. 2012;7(12):e52167.
24. Capper D, Weissert S, Balss J, Habel A, Meyer J, Jäger D, Ackermann U, Tessmer C, Korshunov A, Zentgraf H, Hartmann C, von Deimling A. Characterization of R132H mutation-specific IDH1 antibody binding in brain tumors. Brain Pathol. 2010 Jan;20(1):245-54.
25. Mansouri A, Hachem LD, Mansouri S, Nassiri F, Laperriere NJ, Xia D, Lindeman NI, Wen PY, Chakravarti A, Mehta MP, Hegi ME, Stupp R, Aldape KD, Zadeh G. MGMT promoter methylation status testing to guide therapy for glioblastoma: refining the approach based on emerging evidence and current challenges. Neuro Oncol. 2019 Feb 14;21(2):167-178.
26. Bell EH, Zhang P, Fisher BJ, Macdonald DR, McElroy JP, Lesser GJ, Fleming J, Chakraborty AR, Liu Z, Becker AP, Fabian D, Aldape KD, Ashby LS, Werner-Wasik M, Walker EM, Bahary JP, Kwok Y, Yu HM, Laack NN, Schultz CJ, Gray HJ, Robins HI, Mehta MP, Chakravarti A. Association of MGMT Promoter Methylation Status With Survival Outcomes in Patients With High-Risk Glioma Treated With Radiotherapy

and Temozolomide: An Analysis From the NRG Oncology/RTOG 0424 Trial. JAMA Oncol. 2018 Oct 1;4(10):1405-1409.

27. Arora I, Gurav M, Rumde R, Dhanavade S, Kadam V, Kurani H, Shetty O, Goda JS, Shetty P, Moiyadi A, Gupta T, Jalali R, Epari S. MGMT gene promoter methylation and its correlation with clinicopathological parameters in glioblastomas. Neurol India. 2018 Jul-Aug;66(4):1106-1114.
28. van den Bent MJ, Chang SM. Grade II and III Oligodendroglioma and Astrocytoma. Neurol Clin. 2018 Aug;36(3):467-484.
29. van den Bent MJ, Smits M, Kros JM, Chang SM. Diffuse Infiltrating Oligodendroglioma and Astrocytoma. J Clin Oncol. 2017 Jul 20;35(21):2394-2401.
30. Shirahata M, Ono T, Stichel D, Schrimpf D, Reuss DE, Sahm F, Koelsche C, Wefers A, Reinhardt A, Huang K, Sievers P, Shimizu H, Nanjo H, Kobayashi Y, Miyake Y, Suzuki T, Adachi JI, Mishima K, Sasaki A, Nishikawa R, Bewerunge-Hudler M, Ryzhova M, Absalyamova O, Golanov A, Sinn P, Platten M, Jungk C, Winkler F, Wick A, Hänggi D, Unterberg A, Pfister SM, Jones DTW, van den Bent M, Hegi M, French P, Baumert BG, Stupp R, Gorlia T, Weller M, Capper D, Korshunov A, Herold-Mende C, Wick W, Louis DN, von Deimling A. Novel, improved grading system(s) for IDH-mutant astrocytic gliomas. Acta Neuropathol. 2018 Jul;136(1):153-166.
31. Camelo-Piragua S, Jansen M, Ganguly A, Kim JC, Cosper AK, Dias-Santagata D, Nutt CL, Iafrate AJ, Louis DN. A sensitive and specific diagnostic panel to distinguish diffuse astrocytoma from astrocytosis:

chromosome 7 gain with mutant isocitrate dehydrogenase 1 and p53. J Neuropathol Exp Neurol. 2011 Feb;70(2):110-5.

32. Christians A, Adel-Horowski A, Banan R, Lehmann U, Bartels S, Behling F, Barrantes-Freer A, Stadelmann C, Rohde V, Stockhammer F, Hartmann C. The prognostic role of IDH mutations in homogeneously treated patients with anaplastic astrocytomas and glioblastomas. Acta Neuropathol Commun. 2019 Oct 17;7(1):156.
33. Grimm SA, Chamberlain MC. Anaplastic astrocytoma. CNS Oncol. 2016 Jul;5(3):145-57.
34. Tirrò E, Massimino M, Broggi G, Romano C, Minasi S, Gianno F, Antonelli M, Motta G, Certo F, Altieri R, Manzella L, Caltabiano R, Barbagallo GMV, Buttarelli FR, Magro G, Giangaspero F, Vigneri P. A Custom DNA-Based NGS Panel for the Molecular Characterization of Patients With Diffuse Gliomas: Diagnostic and Therapeutic Applications. Front Oncol. 2022 Mar 17;12:861078. doi: 10.3389/fonc.2022.861078.
35. Broggi G, Barresi V. Assessment of CDKN2A/B homozygous deletion in gliomas: To FISH or not to FISH? J Neuropathol Exp Neurol. 2023 Jul 20;82(8):742-744. doi: 10.1093/jnen/nlad045.
36. Diplas BH, He X, Brosnan-Cashman JA, Liu H, Chen LH, Wang Z, Moure CJ, Killela PJ, Loriaux DB, Lipp ES, Greer PK, Yang R, Rizzo AJ, Rodriguez FJ, Friedman AH, Friedman HS, Wang S, He Y, McLendon RE, Bigner DD, Jiao Y, Waitkus MS, Meeker AK, Yan H. The genomic landscape of TERT promoter wildtype-IDH wildtype glioblastoma. Nat Commun. 2018 May 25;9(1):2087.

37. Burgenske DM, Yang J, Decker PA, Kollmeyer TM, Kosel ML, Mladek AC, Caron AA, Vaubel RA, Gupta SK, Kitange GJ, Sicotte H, Youland RS, Remonde D, Voss JS, Fritcher EGB, Kolsky KL, Ida CM, Meyer FB, Lachance DH, Parney IJ, Kipp BR, Giannini C, Sulman EP, Jenkins RB, Eckel-Passow JE, Sarkaria JN. Molecular profiling of long-term IDH-wildtype glioblastoma survivors. Neuro Oncol. 2019 Nov 4;21(11):1458-1469.
38. Kessler T, Sahm F, Sadik A, Stichel D, Hertenstein A, Reifenberger G, Zacher A, Sabel M, Tabatabai G, Steinbach J, Sure U, Krex D, Grosu AL, Bewerunge-Hudler M, Jones D, Pfister SM, Weller M, Opitz C, Bendszus M, von Deimling A, Platten M, Wick W. Molecular differences in IDH wildtype glioblastoma according to MGMT promoter methylation. Neuro Oncol. 2018 Feb 19;20(3):367-379.
39. Le Rhun E, Preusser M, Roth P, Reardon DA, van den Bent M, Wen P, Reifenberger G, Weller M. Molecular targeted therapy of glioblastoma. Cancer Treat Rev. 2019 Nov;80:101896.
40. Korshunov A, Casalini B, Chavez L, Hielscher T, Sill M, Ryzhova M, Sharma T, Schrimpf D, Stichel D, Capper D, Reuss DE, Sturm D, Absalyamova O, Golanov A, Lambo S, Bewerunge-Hudler M, Lichter P, Herold-Mende C, Wick W, Pfister SM, Kool M, Jones DTW, von Deimling A, Sahm F. Integrated molecular characterization of IDH-mutant glioblastomas. Neuropathol Appl Neurobiol. 2019 Feb;45(2):108-118.
41. Korshunov A, Casalini B, Chavez L, Hielscher T, Sill M, Ryzhova M, Sharma T, Schrimpf D, Stichel D, Capper D, Reuss DE, Sturm D,

Absalyamova O, Golanov A, Lambo S, Bewerunge-Hudler M, Lichter P, Herold-Mende C, Wick W, Pfister SM, Kool M, Jones DTW, von Deimling A, Sahm F. Integrated molecular characterization of IDH-mutant glioblastomas. Neuropathol Appl Neurobiol. 2019 Feb;45(2):108-118.

42. Li KK, Shi ZF, Malta TM, Chan AK, Cheng S, Kwan JSH, Yang RR, Poon WS, Mao Y, Noushmehr H, Chen H, Ng HK. Identification of subsets of IDH-mutant glioblastomas with distinct epigenetic and copy number alterations and stratified clinical risks. Neurooncol Adv. 2019 May-Dec;1(1):vdz015
43. Lu VM, O'Connor KP, Shah AH, Eichberg DG, Luther EM, Komotar RJ, Ivan ME. The prognostic significance of CDKN2A homozygous deletion in IDH-mutant lower-grade glioma and glioblastoma: a systematic review of the contemporary literature. J Neurooncol. 2020 Jun;148(2):221-229.
44. Wesseling P, van den Bent M, Perry A. Oligodendroglioma: pathology, molecular mechanisms and markers. Acta Neuropathol. 2015 Jun;129(6):809-27.
45. Van den Bent MJ, Reni M, Gatta G, Vecht C. Oligodendroglioma. Crit Rev Oncol Hematol. 2008 Jun;66(3):262-72.
46. Engelhard HH, Stelea A, Mundt A. Oligodendroglioma and anaplastic oligodendroglioma: clinical features, treatment, and prognosis. Surg Neurol. 2003 Nov;60(5):443-5.
47. Engelhard HH, Stelea A, Cochran EJ. Oligodendroglioma: pathology and molecular biology. Surg Neurol. 2002 Aug;58(2):111-7; discussion 117.

48. Bailey P, Cushing H (1926) A Classification of Tumors of the Glioma Group on a Histogenetic basis with a Correlation Study of Prognosis. Lippincott, Philadelphia.
49. Tan AP, Tan CL, Pang YH, Kei PL. Anaplastic Oligodendroglioma with Transdural Extension. World Neurosurg. 2019 Oct;130:10-12.
50. Rosenberg S, Ducray F, Alentorn A, Dehais C, Elarouci N, Kamoun A, Marie Y, Tanguy ML, De Reynies A, Mokhtari K, Figarella-Branger D, Delattre JY, Idbaih A; POLA Network. Machine Learning for Better Prognostic Stratification and Driver Gene Identification Using Somatic Copy Number Variations in Anaplastic Oligodendroglioma. Oncologist. 2018 Dec;23(12):1500-1510.
51. Dubbink HJ, Atmodimedjo PN, Kros JM, French PJ, Sanson M, Idbaih A, Wesseling P, Enting R, Spliet W, Tijssen C, Dinjens WN, Gorlia T, van den Bent MJ. Molecular classification of anaplastic oligodendroglioma using next-generation sequencing: a report of the prospective randomized EORTC Brain Tumor Group 26951 phase III trial. Neuro Oncol. 2016 Mar;18(3):388-400.
52. Holdhoff M, Cairncross GJ, Kollmeyer TM, Zhang M, Zhang P, Mehta MP, Werner-Wasik M, Souhami L, Bahary JP, Kwok Y, Hartford AC, Chakravarti A, Yegnasubramanian S, Vogelstein B, Papadopoulos N, Kinzler K, Jenkins RB, Bettegowda C. Genetic landscape of extreme responders with anaplastic oligodendroglioma. Oncotarget. 2017 May 30;8(22):35523-35531.

53. Collins VP, Jones DT, Giannini C. Pilocytic astrocytoma: pathology, molecular mechanisms and markers. Acta Neuropathol. 2015 Jun;129(6):775-88.
54. Lourenço EP, Nzwalo H, Sampaio MR, Varela AV. Pilocytic astrocytoma. BMJ Case Rep. 2016 Mar 31;2016:bcr2015213013.
55. Bond KM, Hughes JD, Porter AL, Orina J, Fang S, Parney IF. Adult Pilocytic Astrocytoma: An Institutional Series and Systematic Literature Review for Extent of Resection and Recurrence. World Neurosurg. 2018 Feb;110:276-283.
56. Bornhorst M, Frappaz D, Packer RJ. Pilocytic astrocytomas. Handb Clin Neurol. 2016;134:329-44.
57. Bikowska-Opalach B, Szlufik S, Grajkowska W, Jozwiak J. Pilocytic astrocytoma: a review of genetic and molecular factors, diagnostic and prognostic markers. Histol Histopathol. 2014 Oct;29(10):1235-48.
58. Gerstner ER, Pajtler KW. Ependymoma. Semin Neurol. 2018 Feb;38(1):104-111.
59. Massimino M, Buttarelli FR, Antonelli M, Gandola L, Modena P, Giangaspero F. Intracranial ependymoma: factors affecting outcome. Future Oncol. 2009 Mar;5(2):207-16.
60. Lester A, McDonald KL. Intracranial ependymomas: molecular insights and translation to treatment. Brain Pathol. 2020 Jan;30(1):3-12.
61. Pagès M, Pajtler KW, Puget S, Castel D, Boddaert N, Tauziède-Espariat A, Picot S, Debily MA, Kool M, Capper D, Sainte-Rose C, Chrétien F, Pfister SM, Pietsch T, Grill J, Varlet P, Andreiuolo F. Diagnostics of pediatric

supratentorial RELA ependymomas: integration of information from histopathology, genetics, DNA methylation and imaging. Brain Pathol. 2019 May;29(3):325-335.

62. Gessi M, Giagnacovo M, Modena P, Elefante G, Gianno F, Buttarelli FR, Arcella A, Donofrio V, Diomedi Camassei F, Nozza P, Morra I, Massimino M, Pollo B, Giangaspero F, Antonelli M. Role of Immunohistochemistry in the Identification of Supratentorial C11ORF95-RELA Fused Ependymoma in Routine Neuropathology. Am J Surg Pathol. 2019 Jan;43(1):56-63.
63. Gessi M, Capper D, Sahm F, Huang K, von Deimling A, Tippelt S, Fleischhack G, Scherbaum D, Alfer J, Juhnke BO, von Hoff K, Rutkowski S, Warmuth-Metz M, Chavez L, Pfister SM, Pietsch T, Jones DT, Sturm D. Evidence of H3 K27M mutations in posterior fossa ependymomas. Acta Neuropathol. 2016 Oct;132(4):635-7.
64. Gessi M, Kuchelmeister K, Lauriola L, Pietsch T. Rare histological variants in ependymomas: histopathological analysis of 13 cases. Virchows Arch. 2011 Oct;459(4):423-9.
65. Massimino M, Barretta F, Modena P, Witt H, Minasi S, Pfister SM, Pajtler KW, Antonelli M, Gandola L, Garrè ML, Bertin D, Mastronuzzi A, Mascarin M, Quaglietta L, Viscardi E, Sardi I, Ruggiero A, Pollo B, Buccoliero A, Boschetti L, Schiavello E, Chiapparini L, Erbetta A, Morra I, Gessi M, Donofrio V, Patriarca C, Giangaspero F, Johann P, Buttarelli FR. The AIEOP 2nd series of children and adolescents intracranial

Ependymoma. An integrated molecular and clinical characterization with a long-term follow-up. Neuro Oncol. 2020 Nov 2:noaa257.

66. Memczak S., Jens M., Elefsinioti A., Torti F., Krueger J., Rybak A., Maier L., Mackowiak S.D., Gregersen L.H., Munschauer M., et al. Circular RNAs are a large class of animal RNAs with regulatory potency. Nature. 2013;495:333–338.
67. Ebbesen KK, Hansen TB, Kjems J. Insights into circular RNA biology. RNA Biol. 2017 Aug 3;14(8):1035-1045.
68. Barbagallo D, Caponnetto A, Cirnigliaro M, Brex D, Barbagallo C, D'Angeli F, Morrone A, Caltabiano R, Barbagallo GM, Ragusa M, Di Pietro C, Hansen TB, Purrello M. CircSMARCA5 Inhibits Migration of Glioblastoma Multiforme Cells by Regulating a Molecular Axis Involving Splicing Factors SRSF1/SRSF3/PTB. Int J Mol Sci. 2018 Feb 6;19(2):480.
69. Barbagallo D, Caponnetto A, Brex D, Mirabella F, Barbagallo C, Lauretta G, Morrone A, Certo F, Broggi G, Caltabiano R, Barbagallo GM, Spina-Purrello V, Ragusa M, Di Pietro C, Hansen TB, Purrello M. CircSMARCA5 Regulates VEGFA mRNA Splicing and Angiogenesis in Glioblastoma Multiforme Through the Binding of SRSF1. Cancers (Basel). 2019 Feb 7;11(2):194.
70. Zhou X, Wang R, Li X, Yu L, Hua D, Sun C, Shi C, Luo W, Rao C, Jiang Z, Feng Y, Wang Q, Yu S. Splicing factor SRSF1 promotes gliomagenesis via oncogenic splice-switching of MYO1B. J Clin Invest. 2019 Feb 1;129(2):676-693.

71. Ishizawa K, Komori T, Shimada S, Hirose T. Olig2 and CD99 are useful negative markers for the diagnosis of brain tumors. Clin Neuropathol. 2008 May-Jun;27(3):118-28.
72. Otero JJ, Rowitch D, Vandenberg S. OLIG2 is differentially expressed in pediatric astrocytic and in ependymal neoplasms. J Neurooncol. 2011 Sep;104(2):423-38.
73. Broggi G, Salvatorelli L, Barbagallo D, Certo F, Altieri R, Tirrò E, Massimino M, Vigneri P, Guadagno E, Maugeri G, D'Agata V, Musumeci G, Ragusa M, Barbagallo GMV, Russo D, Caltabiano R. Diagnostic Utility of the Immunohistochemical Expression of Serine and Arginine Rich Splicing Factor 1 (SRSF1) in the Differential Diagnosis of Adult Gliomas. Cancers (Basel). 2021 Apr 26;13(9):2086. doi: 10.3390/cancers13092086.